



RESEARCH ARTICLE

10.1029/2023JD038557

Day-To-Day Quantification of Changes in Global Lightning Activity Based on Schumann Resonances

Key Points:

- Daily average Schumann resonance intensity is a quasi-global invariant quantity that shows good agreement with global daily stroke rates and thunder hours
- Global lightning activity can vary by a factor of 2–3 on a 3–5 day timescale which could be attributed to cold air outbreaks
- Currently available technology does not allow the detailed quantitative evaluation of lightning activity on continental scales

Supporting Information:

Supporting Information may be found in the online version of this article.

Correspondence to:

T. Bozóki,
Bozoki.Tamas@epss.hu

Citation:

Bozóki, T., Sántori, G., Williams, E., Guha, A., Liu, Y., Steinbach, P., et al. (2023). Day-to-day quantification of changes in global lightning activity based on Schumann resonances. *Journal of Geophysical Research: Atmospheres*, 128, e2023JD038557. <https://doi.org/10.1029/2023JD038557>

Received 20 JAN 2023
Accepted 9 MAY 2023

T. Bozóki^{1,2,3} , G. Sántori¹ , E. Williams⁴, A. Guha⁵, Y. Liu⁴ , P. Steinbach^{3,6} , A. Leal^{7,8} , M. Herein^{1,9,10} , M. Atkinson¹¹, C. D. Beggan¹² , E. DiGangi¹³ , A. Koloskov^{14,15}, A. Kulak¹⁶, J. LaPierre¹³, D. K. Milling¹⁷, J. Mlynarczyk¹⁶ , A. Neska¹⁸, A. Potapov¹⁹ , T. Raita²⁰, R. Rawat²¹, R. Said²² , A. K. Sinha²³, and Y. Yampolski²⁴

¹Institute of Earth Physics and Space Science (EPSS), Sopron, Hungary, ²Department of Optics and Quantum Electronics, University of Szeged, Szeged, Hungary, ³Department of Geophysics and Space Science, Eötvös Loránd University, Budapest, Hungary, ⁴Parsons Laboratory, Massachusetts Institute of Technology, Cambridge, MA, USA, ⁵Department of Physics, Tripura University, Agartala, India, ⁶ELKH-ELTE Space Research Group, Budapest, Hungary, ⁷Department of Physics and Langmuir Laboratory, New Mexico Institute of Mining and Technology, Socorro, NM, USA, ⁸Graduate Program in Electrical Engineering, Federal University of Pará, Belem, Brazil, ⁹ELKH-ELTE Theoretical Physics Research Group, Budapest, Hungary, ¹⁰Department of Theoretical Physics, Institute of Physics and Astronomy, Eötvös Loránd University, Budapest, Hungary, ¹¹HeartMath Institute, Boulder Creek, CA, USA, ¹²British Geological Survey, Edinburgh, UK, ¹³Advanced Environmental Monitoring (AEM), Germantown, MD, USA, ¹⁴Department of Physics, University of New Brunswick, Fredericton, NB, Canada, ¹⁵State Institution National Antarctic Scientific Center of Ukraine, Kyiv, Ukraine, ¹⁶Institute of Electronics, AGH University of Science and Technology, Krakow, Poland, ¹⁷Department of Physics, University of Alberta, Edmonton, AB, Canada, ¹⁸Institute of Geophysics, Polish Academy of Sciences, Warsaw, Poland, ¹⁹Institute of Solar-Terrestrial Physics SB RAS, Irkutsk, Russia, ²⁰Sodankylä Geophysical Observatory, University of Oulu, Sodankylä, Finland, ²¹Indian Institute of Geomagnetism, Navi Mumbai, India, ²²Vaisala, Louisville, CO, USA, ²³Department of Physics, School of Science, University of Bahrain, Zallaq, Bahrain, ²⁴Institute of Radio Astronomy, National Academy of Sciences of Ukraine, Kharkiv, Ukraine

Abstract The importance of lightning has long been recognized from the point of view of climate-related phenomena. However, the detailed investigation of lightning on global scales is currently hindered by the incomplete and spatially uneven detection efficiency of ground-based global lightning detection networks and by the restricted spatio-temporal coverage of satellite observations. We are developing different methods for investigating global lightning activity based on Schumann resonance (SR) measurements. SRs are global electromagnetic resonances of the Earth-ionosphere cavity maintained by the vertical component of lightning. Since charge separation in thunderstorms is gravity-driven, charge is typically separated vertically in thunderclouds, so every lightning flash contributes to the measured SR field. This circumstance makes SR measurements very suitable for climate-related investigations. In this study, 19 days of global lightning activity in January 2019 are analyzed based on SR intensity records from 18 SR stations and the results are compared with independent lightning observations provided by ground-based (WWLLN, GLD360, and ENTLN) and satellite-based (GLM, LIS/OTD) global lightning detection. Daily average SR intensity records from different stations exhibit strong similarity in the investigated time interval. The inferred intensity of global lightning activity varies by a factor of 2–3 on the time scale of 3–5 days which we attribute to continental-scale temperature changes related to cold air outbreaks from polar regions. While our results demonstrate that the SR phenomenon is a powerful tool to investigate global lightning, it is also clear that currently available technology limits the detailed quantitative evaluation of lightning activity on continental scales.

Plain Language Summary Lightning is recognized as a climate variable indicating the changing climate of the Earth. Surface temperature changes on the order of 1°C can result in a significant change in lightning frequency. Lightning activity is monitored on a global scale by satellites and by ground-based global lightning detection networks. However, the detection efficiency of these available technologies is limited which restricts the investigation of global lightning activity especially on the day-to-day time scale. In this study, we propose an alternative method to monitor day-to-day changes in global lightning activity based on Schumann resonance measurements and thus we compare SR-based observations with available global lightning monitoring techniques. We show that the overall intensity of global lightning activity can vary considerably (by a factor of 2–3) within a few days, further motivating our efforts to monitor such changes and understand

© 2023. The Authors.

This is an open access article under the terms of the [Creative Commons Attribution-NonCommercial-NoDerivs License](https://creativecommons.org/licenses/by/4.0/), which permits use and distribution in any medium, provided the original work is properly cited, the use is non-commercial and no modifications or adaptations are made.

their causes. It is also clear from our study that new methods are needed to quantitatively characterize continental-scale lightning activity.

1. Introduction

Global lightning activity is known as an essential indicator of global climate and has the potential to reveal important consequences of climate change (Aich et al., 2018). The main argument behind this statement is the nonlinear relation between lightning activity and surface temperature (Williams, 1992). Temperature perturbations on the order of 1°C have pronounced local effects on cloud electrification which can result in a significant change in lightning frequency (up to 10% per 1°C) depending on the time scale investigated (Williams, 2020; Williams et al., 2023). A dramatic increase (up to 300%) of lightning has been revealed at Arctic latitudes which correlates well with the global temperature anomaly indicating a temperature enhancement from 0.65°C to 0.95°C in the Arctic region from 2010 to 2020 (Holzworth et al., 2021). However, there is some uncertainty in this result, which is related to the time-dependent detection efficiency of the applied lightning detection network (Williams et al., 2023). In a more global context it has been shown that the global lightning record from the Lightning Imaging Sensor (LIS) shows statistically flat behavior over the 2002–2013 period, which is often termed a “hiatus” in global warming with flat temperature trend (Williams et al., 2019). Recently, the radiated energy of global lightning activity has been described using a rigorous quantum physics framework, which is expected to help better understand the impact of climate change on global lightning and the Earth's atmosphere in general (Füllekrug, 2021a).

Lightning is not only an indicator but also a driver of climate change by producing strong greenhouse gases (Price et al., 1997; Schumann & Huntrieser, 2007). A strong correlation has also been found between convective intensity and upper tropospheric water vapor, one further key element of Earth's climate, and lightning is related to convective intensity (Plotnik et al., 2021; Price, 2000). This result underlines that thunderstorms play an important role in the global redistribution of water, a key mediator of both short and long wavelength radiation (Williams, 2005). All these aspects motivate efforts to monitor the long-term characteristics of lightning on local, regional, and global scales, including the stroke occurrence rate, the average charge transfer, the flash intensity and extent, as well as the distribution of thunderstorm-affected areas, lightning hotspots and lightning superbolts (e.g., Albrecht et al., 2016; Beirle et al., 2014; Blakeslee et al., 2014; Blakeslee et al., 2020; Boldi et al., 2018; Cecil et al., 2015; Chronis & Koshak, 2017; Holzworth et al., 2019; Lyons et al., 2020; Peterson et al., 2021).

About 50 lightning flashes occur every second at any given time on Earth (Christian et al., 2003) and this rate can vary by as much as 10%–20% on different time scales (Aich et al., 2018; Albrecht et al., 2016; Cecil et al., 2014; Williams, 2020). Optical detection carried out by satellites provides one way to study lightning activity on global scales. Lightning detection from Low Earth Orbit (LEO), like the Lightning Imaging Sensor (LIS) onboard the Tropical Rainfall Measuring Mission (TRMM, 1997–2015, Christian et al., 2003) and the International Space Station (ISS, February 2017–present, Blakeslee et al., 2020), lays the foundations for essential statistical studies. The limitation of this technique is that continuous monitoring of a specific thunderstorm area is not possible as lightning strokes outside the suborbital swath are not detected. On the other hand, lightning detection from Geostationary Earth Orbit (GEO), like the Geostationary Lightning Mapper (GLM) instrument onboard the GOES-R series satellites (Goodman et al., 2013) and the Lightning Mapping Imager (LMI) instrument onboard the FengYun-4A satellite (Yang et al., 2017), provides continuous lightning monitoring for a given longitudinal sector. Although the appearance of these satellite-based methods represent a major advance for lightning detection on global scales, the current lack of global coverage (i.e., all longitudinal sectors) and the general limitations of optical lightning detection (e.g., the dependence on cloud thickness and time of the day) call for alternative approaches.

Ground-based monitoring of global lightning activity represents another possibility for lightning research, with simultaneous world-wide coverage and with less elaborate and costly infrastructure. Global ground-based lightning monitoring utilizes the electromagnetic (EM) signal emitted by lightning for detection. As the power radiated by lightning peaks in the Very Low Frequency (VLF, 3–30 kHz) band (Wait, 1970) global lightning activity can be monitored with a network of VLF receivers. Such networks require hundreds of VLF (or broadband) receiver stations to achieve global coverage. The World Wide Lightning Location Network (<http://wwlln.net>) is a collaboration among over 50 universities and institutions for providing lightning locations based on this technique. Currently, at least two additional global lightning detection networks are in operation: the Global Lightning Detection Network (GLD360) of Vaisala and Earth Networks Total Lightning Network (ENTLN).

The detection efficiency of global lightning detection networks is a key issue for their applicability in climate research (Virts et al., 2013). However, the detection efficiencies are generally unknown, partly because of the lack of a reliable reference data set (Burgesser, 2017) and partly because of the confidentiality of this information for commercially-operated networks. Even the locations of receiver stations are known only for the research-oriented WWLLN network. For a one-year period between November 2014 and October 2015, the absolute global detection efficiency of GLD360, ENTLN and WWLLN has been estimated to be 59.8%, 56.8%, and 7.9%, respectively, based on Bayesian analysis (Bitzer & Burchfield, 2016). However, for relatively strong discharges these values are significantly higher (e.g., in the case of the WWLLN this detection efficiency is about 50% based on Hutchins et al., 2012). It is to be emphasized that these detection efficiencies are spatially uneven (see e.g., Hutchins et al., 2012; Marchand et al., 2019; Rudlosky, 2015), which restricts detailed investigation of lightning on global scales and prevents the detailed quantitative comparison of lightning activity on continental scales on time scales ranging from the diurnal to the interannual. One important example of this limitation is that lightning activity in Africa is usually underestimated by these networks as compared to Earth's other two main lightning "chimneys" in the Americas and Asia (Williams & Mareev, 2014). The lower number of receiver stations in the African region is one of the plausible explanations for this observation (Williams & Mareev, 2014). From all these aspects it can be concluded that despite substantial interest in investigating global lightning activity for meteorological/climatological purposes, this endeavor is considerably limited by the vagaries of detection efficiency with available lightning monitoring technologies.

The attenuation of EM waves in the lowest part (<100 Hz) of the Extremely Low Frequency (ELF, 3 Hz–3 kHz) band (in the range of 0.2–0.5 dB/Mm; Chapman et al., 1966; Wait, 1970) is substantially smaller than in the VLF band (in the range of 1–10 dB/Mm; Barr et al., 2000; Hutchins et al., 2013; Taylor, 1960). This fact enables the investigation of global lightning activity with a much lower number of receiver stations (1–20). In the ELF band lightning-radiated EM waves travel a number of times around the globe in the waveguide formed by the Earth's surface and the lower ionosphere before losing most of their energy. The constructive interference of the EM waves propagating in opposite directions (direct and antipodal waves) creates global EM resonances called Schumann resonances (SRs) which can be observed at ~8, ~14, ~20, etc. Hz (Balsler & Wagner, 1960; Galejs, 1972; Madden & Thompson, 1965; Nickolaenko & Hayakawa, 2002; Price, 2016; Schumann, 1952; Wait, 1970). While SR frequencies can be used to deduce temporal changes in the global displacement and migration of lightning activity (e.g., Koloskov et al., 2020; Satori, 1996; Satori & Zieger, 1999; Satori & Zieger, 2003) as well as in the areal compactness of global lightning (Nickolaenko & Rabinowicz, 1995; Nickolaenko et al., 1998; Satori & Zieger, 2003), SR intensities are known to indicate the overall intensity of global lightning activity (Boldi et al., 2018; Clayton & Polk, 1977; Heckman et al., 1998; Nickolaenko & Hayakawa, 2002; Sentman & Fraser, 1991). Several works have already shown that variations of SRs are consistent with climatological lightning distributions provided by satellite-based lightning detection (e.g., Boldi et al., 2018; Füllekrug, 2021b; Satori et al., 2009). SRs represent the transverse magnetic (TM) resonance mode of the Earth-ionosphere cavity resonator, which can be excited by vertical lightning discharges (Jackson, 1975). Since the ice-based process of charge separation in thunderstorms is gravity-driven, charge is basically separated vertically in a thundercloud, so every lightning flash in the atmosphere (intracloud and cloud-to-ground alike) is guaranteed to contribute to the SR intensity. This makes SR observations well-suited for climate-related studies (see e.g., Satori, 1996; Satori et al., 2009; Williams, 2020; Williams et al., 2021).

The AC global electric circuit as manifest in Schumann resonances is a technically-involved electromagnetic phenomenon (Madden & Thompson, 1965), standing in sharp contrast with the simpler treatment of the DC global electric circuit, which is modeled as a giant spherical capacitor (Haldoupis et al., 2017) characterized by a single scalar: the ionospheric potential (Markson, 2007). The long-standing quest for an equivalent scalar quantity for SRs was initiated by Sentman and Fraser (1991) as the sum of magnetic modal intensities. The aim here was to average out the complicated source-receiver distance effects to approximate the global behavior by introducing a globally invariant SR-based quantity. Their three-decade-old suggestion is tested in the present work in an unprecedented way.

The understanding of the response of global lightning to temperature on short time scales has been stymied historically by the traditional monthly resolution of data sets on global surface air temperature (e.g., Hansen & Lebedeff, 1987). In this study, the global land surface temperature and lightning activity are analyzed with daily resolution. This investigation has the potential to reveal important variability of the climate system that could change over time as a result of climate change. On this time scale, global effects of cold air outbreaks, when

Table 1
Detailed Information on the 18 SR Stations Used in the Study

Station	Code	Country	Latitude (°N)	Longitude (°E)	Sampling (Hz)
Alberta	ALB	Canada	51.89	-111.47	130.2
Bharati	BRT	Antarctica	-69.41	76.19	256
Boulder Creek	BOU	USA	37.19	-122.12	130.2
Eskdalemuir	ESK	UK	55.29	-3.17	100
Fort Churchill	FCHU	Canada	58.76	-94.08	100
Hofuf	HOF	Saudi Arabia	25.94	48.95	130.2
Hornsund	HRN	Norway	77.0	15.6	100
Hugo	HUG	USA	38.89	-103.40	887.8
Hylaty	HYL	Poland	49.19	22.55	887.8
Kevo	KEV	Finland	69.75	27.02	250
Kilpisjarvi	KIL	Finland	69.05	20.79	250
Ministik Lake	MSTK	Canada	53.35	-112.97	100
Mondy	MND	Russia	51.6	100.9	64
Northland	NOR	New Zealand	-35.11	173.49	130.2
Patagonia	PAT	Argentina	-51.59	-69.32	887.8
Shillong	SHI	India	25.6	91.9	64
Sodankyla	SOD	Finland	67.43	26.39	250
Vernadsky	VRN	Antarctica	-65.25	-64.25	320

cold air masses are transported from polar to mid- and low-latitudes, become readily apparent, as will be elaborated on below.

Episodic intrusions of cold air from high latitudes into warmer air at low latitudes have been extensively investigated under the names “cold surges,” “polar air outbreaks,” “cold air outbreaks,” and “freeze events”, and provide a plausible explanation for global temperature perturbations lasting for one to several days. In extreme events, the colder equator-moving air can extend across the equator into the opposite hemisphere and impact the local tropical temperature at the level of 1°C. An excellent summary can be found in Hastenrath (1996). Such events may originate in either northern (Hartjenstein & Block, 1991) or southern hemispheres, but the literature is more abundant in studies in southern hemisphere winter (Kousky, 1979; Lanfredi & Camargo, 2018; Lupo et al., 2001; Marengo et al., 1997; Prince & Evans, 2018). The reason for this imbalanced attention may arise because the Antarctic winter air is colder than Arctic air, and because the protection of coffee plantations during freeze events in Brazil is of substantial economic interest (Marengo et al., 1997). The longitudinally-confined nature of the polar outbreaks results in lower-latitude impacts that are sometimes confined to individual continental chimneys (America, Africa, Southeast Asia), with corresponding collections of events in Prince and Evans (2018), Crossett and Metz (2017), Murakami (1979), respectively, or to broader impacts affecting multiple chimneys (Metz et al., 2013) as the equatorward-moving cold air also advects eastward.

In this study, we analyze global lightning activity from 13 to 31 January 2019 based on SR intensity records from 18 SR stations around the globe and compare the results with lightning observations provided by independent ground-based (WWLLN, GLD360, and ENTLN) and satellite-based (GLM,

LIS/OTD) global lightning detection. The main motivation of this study is (a) to show that global lightning can vary substantially on a day-to-day basis and (b) to demonstrate that SR measurements are very well-suited to monitor and investigate these day-to-day variations. It is to be highlighted that this is the first study to analyze such a large number of SR stations simultaneously. We will show that summing the intensity of the first three modes of the two magnetic field components and averaging these values on a daily basis results in a quantity that exhibits very similar (but not exactly identical) behavior at all SR stations studied, and is therefore called a quasi-global invariant. To illustrate the robustness of this quasi-global invariant quantity for characterizing day-to-day changes in global lightning activity, a second time interval (1–31 January 2015) is also investigated (albeit in less detail).

2. Data and Methods

2.1. Data on Schumann Resonances

The most important information about the 18 SR stations used in this study are listed in Table 1 and their locations are shown in Figure 1. All the stations are equipped with a pair of induction coil magnetometers that are in most cases aligned with the local geographical meridian and perpendicular to it, except at the Fort Churchill (FCHU), Ministik Lake (MSTK) and Mondy (MND) stations where they are oriented along the geomagnetic north-south (NS) and east-west (EW) directions. The Alberta (ALB), Boulder Creek (BOU), Hofuf (HOF) and Northland (NOR) stations are operated by the Heartmath Institute (<https://www.heartmath.org/gci/>) and are used mainly to study the relationship between humans and our electromagnetic environment (e.g., Timofejeva et al., 2021). The Bharati (BRT) and Shillong (SHI) stations are operated by the Indian Institute of Geomagnetism. The low resolution (64 Hz) data from the low latitude SHI station in India have been used to study ionospheric Alfvén resonances (IAR) (e.g., Adhitya et al., 2022) while high resolution (256 Hz)

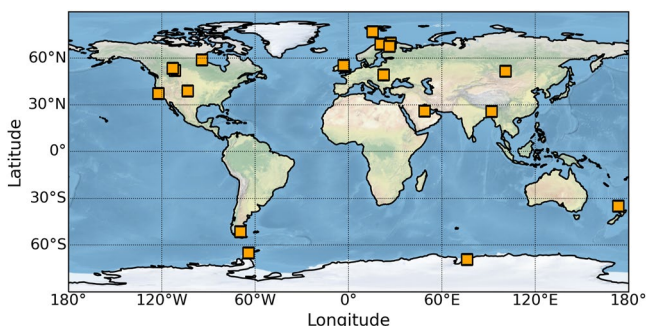


Figure 1. Map showing the locations of the 18 SR stations used in the study (marked by orange squares) and listed in Table 1.

data from the Antarctic BRT station have been used to examine finer structures of electromagnetic ion cyclotron (EMIC) waves (e.g., Kakad et al., 2018; Upadhyay et al., 2022). The Eskdalemuir (ESK) station is operated by the British Geological Survey and is dedicated to study SRs and ionospheric Alfvén resonances (see e.g., Beggan & Musur, 2018; Musur & Beggan, 2019). The Hornsund (HRN) station in Svalbard is maintained by the Institute of Geophysics (Polish Academy of Sciences) and has been used to study SRs for almost two decades (e.g., Neska et al., 2019; Sători et al., 2007). The Mondy (MND) station belongs to the Institute of Solar-Terrestrial Physics (Russian Academy of Sciences). This station has been recently used to investigate globally observable ELF-transients (Marchuk et al., 2022). The Vernadsky (VRN) station in Antarctica is operated by the Institute of Radio Astronomy (National Academy of Sciences of Ukraine) and is one of the most extensively used stations in SR research (e.g., Koloskov et al., 2020; Koloskov et al., 2022; Sători et al., 2016). The Fort Churchill (FCHU) and Ministik Lake (MSTK) stations are part of the CARISMA network (carisma.ca, Mann et al., 2008) operated by the University of Alberta. These stations are mainly used to study EMIC/Pc1 waves (Kim et al., 2018; Matsuda et al., 2021). The Hugo (HUG), Hylaty (HYL) and Patagonia (PAT) stations belong to the World ELF Radiolocation Array (WERA, <http://www.oa.uj.edu.pl/elf/index/projects3.htm>, Kulak et al., 2014) operated by the Krakow ELF group. The primary objective of WERA is to radiolocate and characterize strong lightning discharges from around the world (e.g., Marchenko et al., 2021; Mlynarczyk et al., 2017; Strumik et al., 2021). The Kevo (KEV), Kilpisjärvi (KIL) and Sodankylä (SOD) stations are part of the Finnish pulsation magnetometer chain (<https://www.sgo.fi/Data/Pulsation/pulDescr.php>) operated by the Sodankylä Geophysical Observatory, University of Oulu. Characterization of EMIC/Pc1 waves and monitoring Alfvén resonances is also a primary goal of this network. In a recent study ALB, BOU, HRN and ESK stations have been utilized to investigate the evolution of continental-scale lightning activity on the timescale of the El Niño–Southern Oscillation (ENSO) (Williams et al., 2021). In another work, the long-term changes in the properties of the Earth-ionosphere waveguide have been analyzed based on the HRN, ESK, SHI and VRN stations (Bozóki et al., 2021). The analyzed period of the present study (13–31 January 2019) was selected based on the availability of data from all the stations listed. The only exception is Mondy (MND) from where data are available only in the 15–30 January period. For the analysis of the second time interval (1–31 January 2015), a smaller number of receivers were considered and only ALB, BOU, HRN and NOR stations were used.

In the following we describe how to obtain the quasi-global invariant quantity from SR measurements. All the raw SR time series were processed in the same way. First, standardized one-hour time series have been generated from raw data files with different formats. In this step, the measured data were filtered using a finite impulse response (FIR) bandpass filter, which also corrected for the amplitude response of the recording systems. For the Heartmath stations (ALB, BOU, HOF, NOR), the amplitude-response function is flat in the SR band, so no correction was applied. For the stations of the Finnish pulsation magnetometer chain (KEV, KIL, SOD), the amplitude response of the measuring system is not known. For the WERA stations (HUG, HYL, PAT) a color noise ($1/f$ type noise) appears in the measurements (see Figure 2 in Mlynarczyk et al., 2017) which cannot be corrected by the amplitude response function, so no correction was applied. Based on the bandwidths of the measuring systems and the available information about the amplitude responses, the bandpasses of the FIR filters have been chosen to be 2–45 Hz for the ALB, BOU, ESK, HOF, HRN, HUG, HYL, NOR, PAT, and VRN stations, 2–31 Hz for the FCHU, MSTK, KEV, KIL, and SOD stations, and 2–30 Hz for the BRT, MND, and SHI stations. For the three stations with geomagnetic orientation of magnetic coils (FCHU, MSTK, MND) a digital antenna rotation has been applied (Mlynarczyk et al., 2015) when generating the standardized time series in order to transform the records to the geographical main directions.

As the next step in the overall procedure, sanitized power spectral density (PSD) spectra were calculated from the standardized time series based on Welch's method (Welch, 1967). This method estimates the PSD by dividing the data into overlapping segments, determining the PSD of each segment and averaging them. First, spikes larger than 100 pT (in absolute value) were replaced by nans (“not a number”-s) in the time domain to minimize the aliasing effect of regional lightning activity (Tatsis et al., 2021) and exceptionally intense lightning strokes known as Q-bursts (Guha et al., 2017). PSD spectrograms (dynamic spectra) were calculated with a window length (depending on the sampling frequency of the actual station) corresponding to ~ 0.1 Hz frequency resolution and a half-window-length overlap. This step unifies the PSD spectra obtained from stations operating at different sampling frequencies. We refer to one column of the spectrogram (dynamic spectrum) which corresponds to the PSD spectrum of one window as a “spectral segment.” Those windows that contained nans resulted in spectral segments with only nans (usually around 1%–2% of all the spectral segments). Next, narrowband, anthropogenic noises (see e.g., Salinas et al., 2022), identified manually for each station, have been removed from the spectra.

One further sanitation step has been applied based on the spectral power content (SPC) (the sum of PSD values) (Guha et al., 2017) in the lowest part of the spectrum (<6 Hz) and in the SR band (6–30 Hz or 6–40 Hz depending on the bandwidth of the actual station) where segments with SPC greater than the average plus one standard deviation (either below 6 Hz or in the SR band) have been removed. This is a strict criterion but its application results in very clear SR spectrograms characteristic of “background” lightning activity, without the influence of nearby or remote but very powerful lightning. If the relative number of removed spectral segments was greater than 40%, then that hour was labeled “bad quality data” and not used. (This relative number of removed spectral segments is usually between 20% and 30%). Finally, average PSD spectra were calculated for 12-min intervals and the average spectra were interpolated on a unified frequency vector from 6 Hz up to 30/40 Hz with 0.2 Hz frequency resolution. The interpolation removed the gaps related to the removal of narrowband, anthropogenic noises (usually aliasing from power grid frequencies).

As the final step, spectral decomposition (4-parameter Lorentzian fitting) has been applied (Kulak et al., 2006) to extract the magnetic intensity of the first three SR modes. Unlike in Dyrda et al. (2014) (Equation 1) we did not include white and color noise terms in the fitting process except for stations of the WERA network. Our experience was that high quality spectral fits can be obtained without the inclusion of the noise terms. Four/six resonance peaks have been fitted for stations with narrower/wider bandwidth, respectively. Finally, we summed the intensities of the first three resonance modes (~8 Hz, ~14 Hz, ~20 Hz) as the main contributor from each magnetic coil to the quasi-global invariant quantity of central interest in this work.

2.2. Independent Lightning Observations

The characteristics of global lightning activity as inferred from the values of the magnetic SR intensity for the 19-day long period of 13–31 January 2019 are compared with independent lightning observations provided by three global, ground-based lightning monitoring networks: the World Wide Lightning Location Network (WWLLN), the Global Lightning Detection Network (GLD360) and the Earth Networks Total Lightning Network (ENTLN) as well as satellite-based optical lightning observations carried out by the LIS/OTD instruments (climatological) and the Geostationary Lightning Mapper (GLM) onboard the GOES-16 and GOES-17 satellites. The latter instruments provides lightning locations for the American longitudinal sector (i.e., the Western Hemisphere). Two kinds of WWLLN lightning data (RelocB and AE) are available for the study. Algorithms yielding RelocB and AE data are much the same, based on spheric identification in VLF waveforms, determination of times of group arrivals, finding matching pairs, and event localizing. RelocB is the “official” WWLLN data product. The criteria and parametrizing of the spheric identification, and selection of stations taken into account in pairing have been somewhat altered in a newer code (AE), where—semi heuristic—lightning energies are also involved as additional derivatives. Energy is not provided by the RelocB. The altered AE algorithm resulted in minor differences between the two sets of identified lightning. LIS/OTD observations are taken from the $0.5^\circ \times 0.5^\circ$ High Resolution Monthly Climatology (HRMC) data set (Cecil, 2006). It is to be noted that the ground-based/satellite-based observations provide strokes/flashes, respectively.

2.3. Earth Networks Thunder Hour

Earth Networks recently released Thunder Hours, a new data product that is available and freely accessible for climate research purposes from 2014 to date (DiGangi et al., 2022). The Earth Networks Thunder Hour is defined simply as an hour during which thunder can be heard in a particular area (in this case, within a 15 km radius) and is simulated using total lightning data from a combined set of ENTLN- and WWLLN-detected lightning locations called Earth Networks Global Lightning Detection Network (ENGLN). The data set is available in $0.05^\circ \times 0.05^\circ$ spatial resolution and one of its main strengths is that it helps to reduce the influence of detection efficiency on the lightning climatology (DiGangi et al., 2022). In this study we calculate the total daily number of thunder hours for the whole globe and for the three main lightning chimneys, and compare them with the SR-based quasi-global invariant quantity.

2.4. Daily Land-Surface Temperature

Berkeley Earth provides an experimental temperature time series with daily resolution (<https://berkeleyearth.org/data/>) which is called the daily land-surface average anomaly and is produced by the Berkeley Earth averaging method described on their website. In this data set land-surface temperatures are reported as anomalies relative to

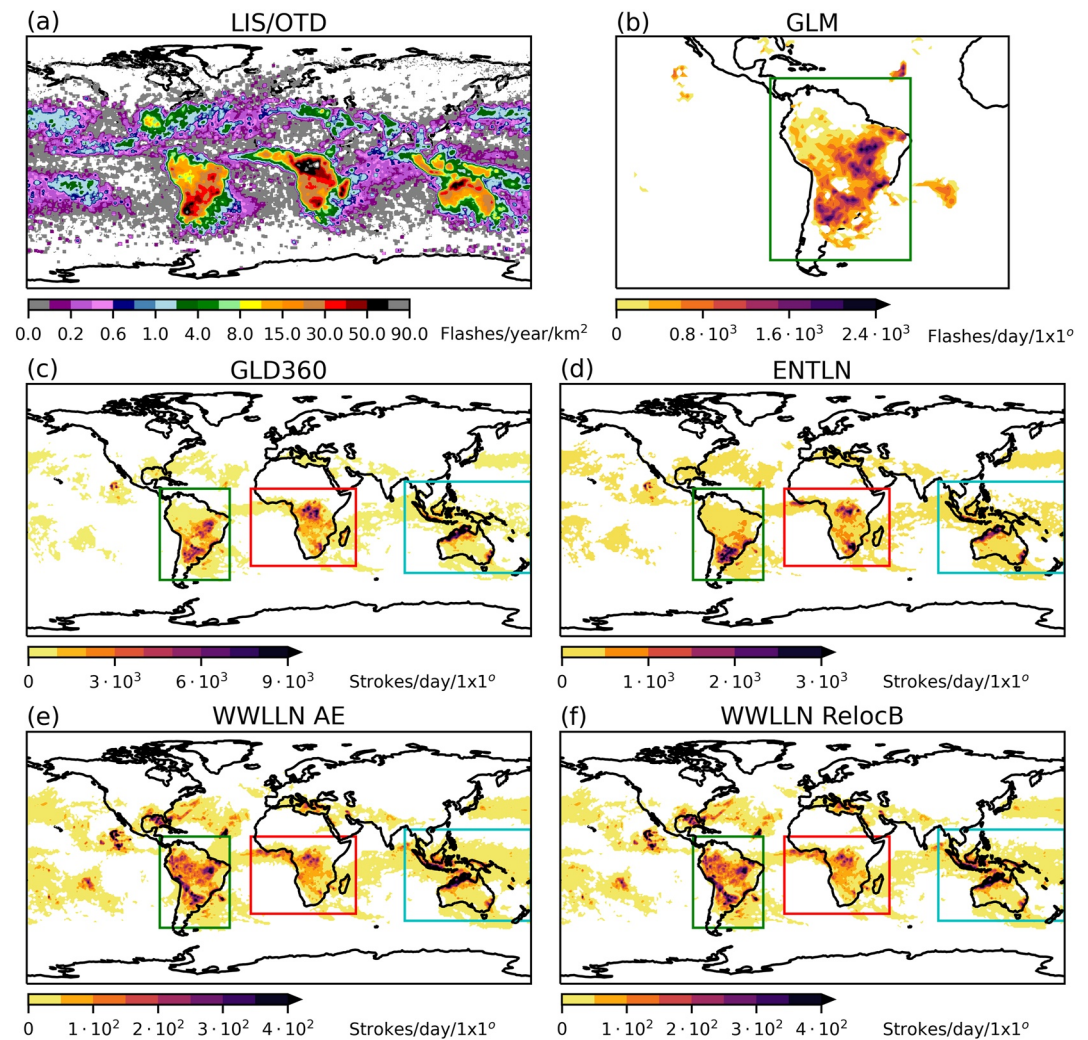


Figure 2. Lightning activity in the 13–31 January 2019 period as seen by different lightning detection methods (except in panel (a) which shows climatological lightning activity for January based on HRMC LIS/OTD observations (Cecil, 2006)). Green (South America), red (Africa) and blue (Maritime Continent) rectangles show those parts of the lightning maps for which stroke/flash numbers and thunder hours are summarized in the chimney-by-chimney analysis (Figures 5, 6b, and 6c). Note that the upper limits of the color scales are different for the different lightning detection methods.

the January 1951–December 1980 average. Although the product is said to be preliminary and could be significantly revised in the future, we consider it a roughly correct indicator of day-to-day changes in the global land temperature.

We also used the CPC (Climate Prediction Center, NOAA) Global Unified Temperature data provided by the NOAA PSL (Physical Science Laboratory, NOAA), Boulder, Colorado, USA (<https://psl.noaa.gov/>) to characterize day-to-day changes in the global land temperature. The Climate Data Operator (CDO, Schulzweida, 2021) has been used to calculate the daily global mean land surface temperature (T_{AVG}) from the 0.5×0.5 Global Daily Gridded Temperature data set (<https://psl.noaa.gov/data/gridded/data.cpc.globaltemp.html>).

3. Results

Figure 2 shows the worldwide lightning activity measured by satellites (Figures 2a and 2b) and by ground-based lightning monitoring networks (Figures 2c–2f). While the LIS/OTD observations show climatological lightning activity for January, all other observations cover the period 13–31 January 2019. In the investigated time interval lightning activity is concentrated in the tropical land regions and in the land areas of the Southern Hemisphere, corresponding to the three main lightning “chimney” regions: the Maritime Continent, Africa and South America.

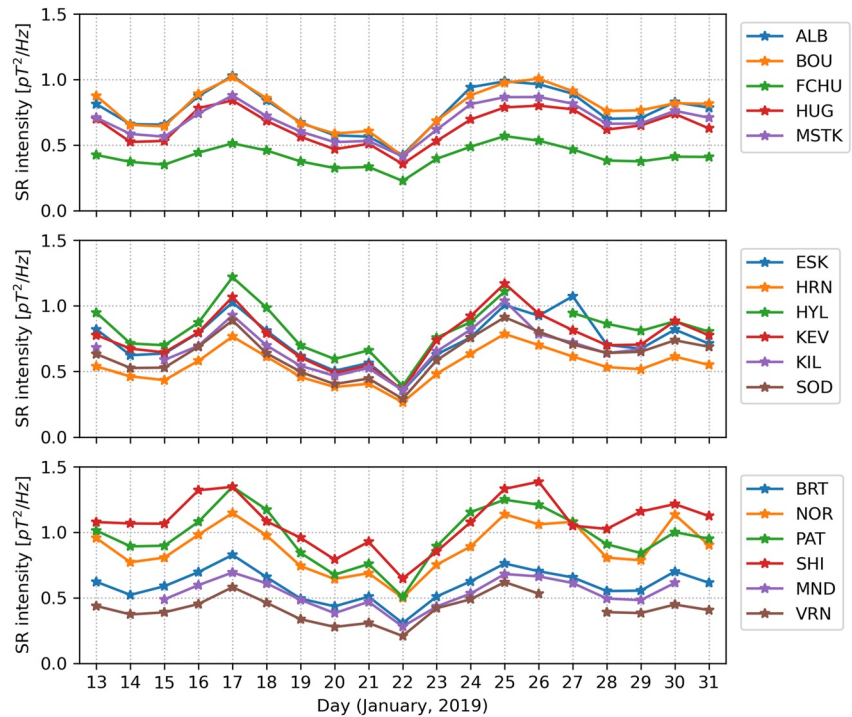


Figure 3. Daily average SR intensity values (the sum of the first three modes and of the two magnetic field components) in the 13–31 January 2019 period. The top panel shows SR intensity records from North America, the middle panel SR intensity records from Europe while the bottom panel SR intensity records from other parts of the globe. A similar behavior of all station records is noted over the 19-day time scale.

This is consistent with the expectation based on solar heating that in Northern Hemispheric winter months global lightning shifts into the Southern Hemisphere (Christian et al., 2003). The LIS/OTD January climatology (Figure 2a) indicates that the African chimney (with largest activity in the Congo basin) is predominant among the three main chimney regions in January. This expectation is not clearly met in the GLD360 (Figure 2c) and ENTLN (Figure 2d) lightning maps and it is definitely not true in case of the WWLLN observations (Figures 2e and 2f). Further differences can be identified among GLD360, ENTLN and WWLLN lightning maps. Strong lightning activity is detected by GLD360 and by WWLLN in the eastern equatorial part of Brazil which is less dominant in the ENTLN data set. On the other hand, ENTLN reports strong lightning activity in the eastern part of South Africa which is less dominant in GLD360 and WWLLN observations. The latter difference between GLD360 and ENTLN could be explained by a higher detection for GLD360 in the Congo basin than that of ENTLN (note the different color scale limits of the maps). The lightning maps also demonstrate that the WWLLN is unique in the sense that it locates intense lightning events globally, far from ground network coverage (e.g., eastward and westward from Central America). The distribution of GLM detected lightning flashes in South America shows the closest similarity with GLD360 observations. These various observations may be summarized with one important conclusion: detection efficiency is a key unknown in the intercomparison of different lightning observations.

Figure 3 shows daily average SR intensity records from 18 stations around the globe. The daily average values are calculated as the sum of the first three SR modes and of the two magnetic field components, in units of pT^2/Hz . The striking similarity between the different records is unambiguous. All of them show a clear maximum on the 17th of January, a well-pronounced minimum on the 22nd of January and a second maximum on the 25–26 of January. A third, smaller maximum can be seen on the 30th of January. SR intensity drops by more than a factor of 2 from 17 to 22 January, that is, in just 5 days. Given the accumulated evidence that lightning intensity is proportional to SR intensity (e.g., Boldi et al., 2018; Clayton & Polk, 1977), the finding suggests a similar reduction in the overall intensity of global lightning activity over this time interval. The possible origins of this large variation on the day-to-day timescale will be addressed in the Discussion. While the general trends in the different records are very similar, the apparent differences in absolute levels are probably connected to the different distances between the active lightning source regions and the SR stations. The figure indicates a trend

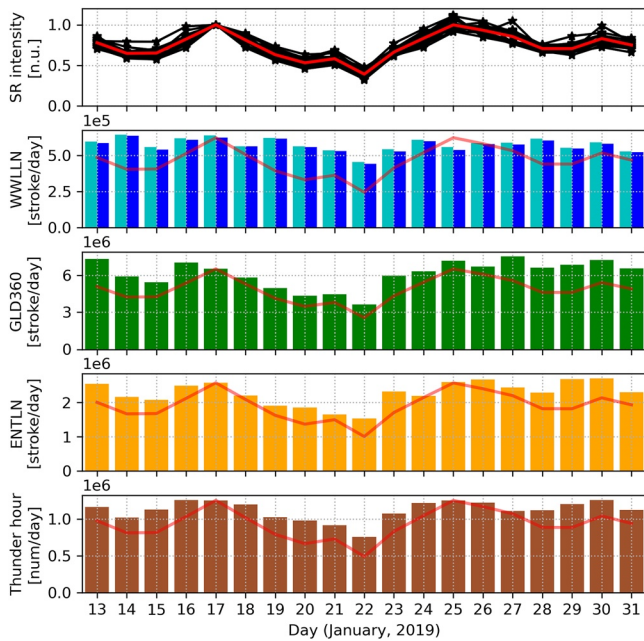


Figure 4. Comparison of normalized daily average SR intensity records (in normalized units) with the total (global) daily stroke rates provided by independent lightning observations (WWLLN, GLD360, ENTLN) and with the total daily numbers of Earth Networks Thunder Hours. In the top subplot black curves correspond to different SR stations while the red curve there shows the average of all records. The scaled version of the latter curve is also shown in the other four subplots. In the second row WWLLN RelocB/AE data are shown in cyan/blue, respectively.

of systematically lower daily average SR intensity values at the polar stations (VRN, BRT, HRN) furthest from the tropical chimney regions, in accordance with the theoretical expectation for wideband SR signals (see Figure 4.24 in Nickolaenko & Hayakawa, 2002). Furthermore, some problems probably also arise with the absolute calibration of the magnetic measurements. That is the reason why we call the daily average SR intensity a *quasi-global* invariant quantity. This could possibly be sorted out by similar intercomparisons in different seasons characterized by different source geometries.

Further comparisons with other measures of global lightning activity over the same 19 day interval are shown in Figure 4. In the top row all the daily average SR intensity records from Figure 3 are displayed but now by applying a normalization with respect to the daily average value on the 17th of January. This step reduces the source-observer distance dependence and calibration problems and makes the high degree of similarity among the different SR intensity records even more obvious. The second, third, fourth and fifth subpanels show the total (global) daily stroke rates provided by the WWLLN (cyan/blue: RelocB/AE), GLD360, and ENTLN as well as the total daily numbers of Earth Networks Thunder Hours. Note that the limits of the y axis are different for the different lightning detection networks. GLD360 reports about 3 times more events than ENTLN and more than 10 times more events than WWLLN. GLD360 and ENTLN data follow the general trend of the normalized average SR intensity record quite well (correlation coefficients are: 0.81 and 0.83 for GLD360 and ENTLN, respectively) and are both superior in this aspect in comparison with WWLLN (correlation coefficients are: 0.52 and 0.48 for WWLLN RelocB and AE, respectively) (Figure S1 in Supporting Information S1). WWLLN RelocB provides about 15% higher daily stroke rates than WWLLN AE but the general trends (day-to-day variations) are very similar in the two data sets. Since the WWLLN is efficient at detecting high amplitude lightning, this observation may suggest that the

day-to-day variation of high amplitude lightning is different from the day-to-day variation of the “average” lightning that maintains SRs. The total daily numbers of Earth Networks Thunder Hours yield the best correlation coefficient with the average SR intensity record: 0.89 (Figure S1 in Supporting Information S1). For more details about the correlation of different data sets we refer to Figure S1 in Supporting Information S1.

It is to be noted that the relative variation of SR intensity records is considerably larger (more than a factor of 2) than that of other lightning records (usually less than a factor of 2). In Table 2 percentage variations of SR intensity are compared with the different lightning observations for those selected days when SR intensity shows the two largest maxima on 17 and 25 January as well as a pronounced minimum on 22 January. The largest percentage increase/decrease appears in the SR intensity and in the GLM records (Table 2) while the smallest increase/decrease in the WWLLN observations.

Figure 5 represents the contributions of individual continental chimneys to the global variations in Figures 3 and 4. It presents SR intensity and independent lightning observations from day-to-day for the three main lightning chimney regions (the Maritime Continent, Africa and South America) in the time intervals (Maritime Continent: 7–11 UT, Africa: 13–17 UT, South America: 18–22 UT) when lightning activity is the strongest in the respective

Table 2
Percentage Changes in Average SR Intensity and in Other Lightning Observations Between 17 and 22 January As Well As Between 22 and 25 January

January days	SR	WWLLN AE	WWLLN RelocB	GLD360	ENTLN	Thunder hour	GLM
17 → 22	−61%	−29%	−29%	−44%	−40%	−40%	−52%
22 → 25	+113%	+36%	+34%	+74%	+43%	+61%	+107%

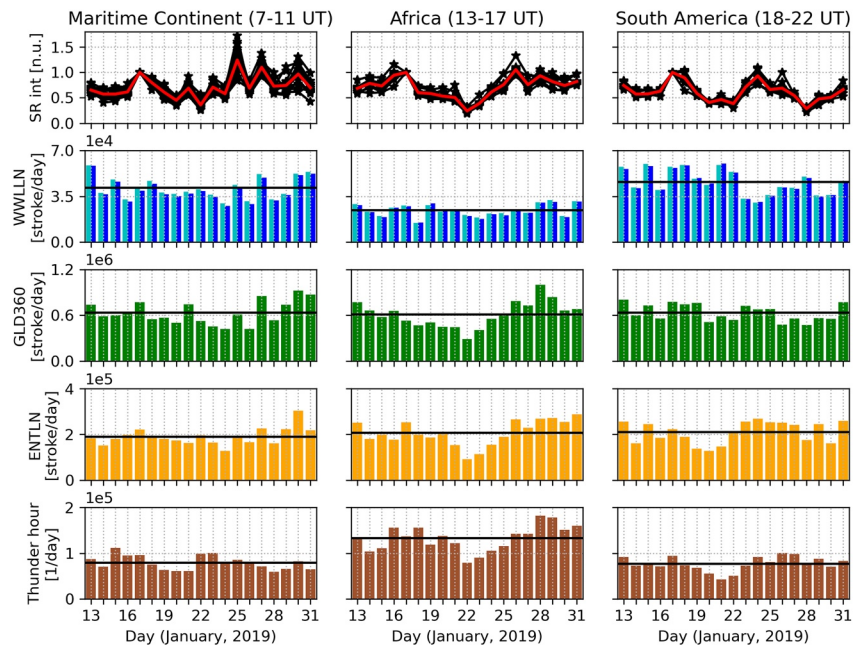


Figure 5. Chimney-by-chimney comparison of normalized average SR intensity records (in normalized units) with stroke rates and thunder hours provided by independent lightning observations (see text for more details). In the top row, black curves correspond to magnetic intensity integrations for different sets of SR stations while the red curve there shows the average of all SR stations in each grouping. In the second, third, fourth and fifth rows, horizontal black lines indicate the mean values of the various plotted quantities.

chimney region (local afternoon hours). The top row shows normalized SR intensity records for selected stations and field components for which the corresponding wave propagation path crosses the actual chimney region (see Figure S2 in Supporting Information S1 for details). On each day SR magnetic intensities are averaged for the first three modes in pT^2/Hz in the time intervals indicated in the top of the figure. The day-to-day changes are different for the three main chimney regions although clear similarities can also be observed between pairs of records. There is again a very high similarity among the SR intensity records from different stations confirming the global representativeness of SR intensity in any time intervals (hours) of a day.

In case of the independent lightning observations (second, third, fourth, and fifth rows of Figure 5), lightning strokes and thunder hours are summarized for the same time intervals as SR intensities within the color-coded rectangles marked in Figure 2. We suppose that these areas contain the main lightning sources for SR intensity. Figure 5 reveals that it is the diminishment of African lightning activity on 22 January that causes the minimum in global lightning activity identified in Figure 4. South American lightning activity is also reduced on this day but this reduction starts a few days earlier. The high correlation between GLD360 and ENTLN for the total (global) daily stroke rates (0.93) drops considerably in this chimney-by-chimney analysis (Maritime Continent: 0.78, Africa: 0.78, South America: 0.34) (Figures S3–S5). For the Maritime Continent and South America, it is GLD360 that yields the highest correlation with the average SR intensity record (0.49 and 0.68, respectively), while for Africa the ENTLN stroke rates show the best performance in this respect (0.77) (Figures S3–S5 in Supporting Information S1). This means that while on the global scale, thunder hours showed the highest correlation with SR, this is not the case on the chimney scale. For more details about the correlation of different data sets on the chimney scale we refer to Figure S3 (Maritime continent), Figure S4 (Africa), and Figure S5 (South America) in Supporting Information S1.

We are also interested in the chimney ranking, that is, the relative strength of the three main lightning chimney regions. Such information on a day-to-day basis may be important for synoptic meteorology and forecasting. In the presented SR intensity records this information is lost when they are normalized with respect to the average value on the 17th of January. Another problem is that SR intensities strongly depend on the source-observer distance, which hinders us from directly utilizing SR intensity records from multiple stations to infer the chimney ranking. We would need to apply an inversion approach to extract this information from the SR records (see e.g., Nelson, 1967; Prácsér et al., 2019; Shvets & Hayakawa, 2011) but this step is out of the scope of the present

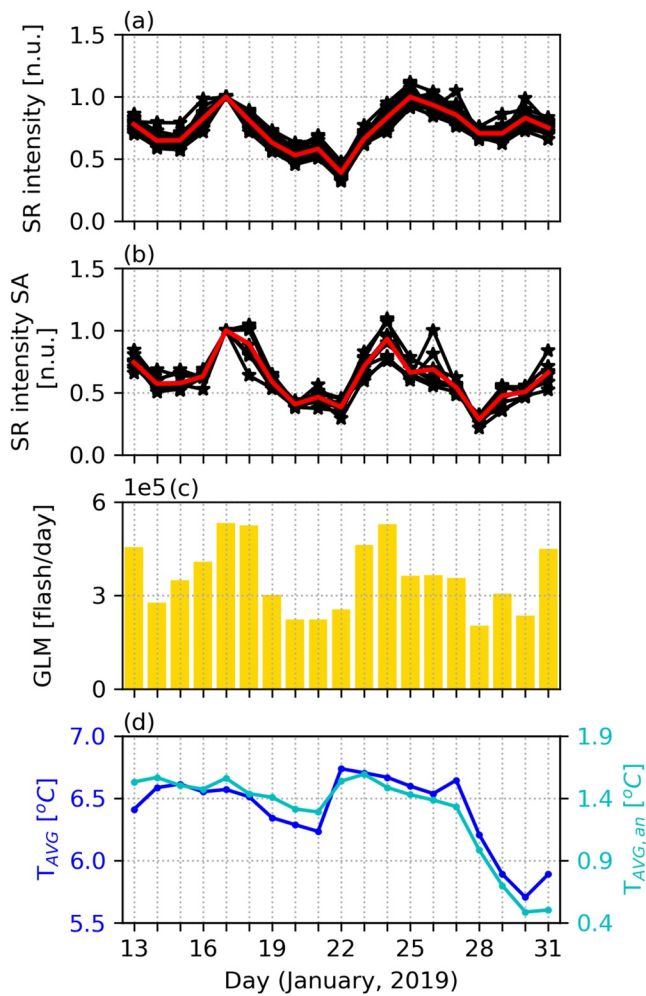


Figure 6. Comparison of (a) normalized daily average SR intensity records (in normalized units) with (b) the normalized average SR intensity records of South America (in normalized units), (c) daily flash rates provided by the GLM instrument and (d) daily global mean land surface temperatures (T_{AVG}) and temperature anomalies ($T_{AVG,an}$). GLM-detected lightning flashes had been summarized within the green rectangle (representing South America) marked in Figure 2.

study. Therefore, we turn to independent lightning observations to investigate the question of chimney ranking. WWLLN indicates that the African chimney has the lowest activity of the three, contrary to the findings of prior studies (e.g., Brooks, 1925), but the African chimney also has the fewest WWLLN receivers of the three. Therefore, this inconsistency could be rooted in detection efficiency issues. The GLD360 and ENTLN daily stroke rates do not show characteristic differences between the three main chimney regions (Figure 5, horizontal black lines). The Asian/African/South American chimneys are the most powerful on 10/5/4 days in the GLD360 data set and on 7/9/3 days in the ENTLN data set, respectively. On the other hand, thunder hours show the clear dominance of the African lightning chimney in accordance with LIS/OTD lightning climatology (Figure 2a). From all these results it is clear that the available lightning monitoring techniques do not provide a consistent and reliable ranking of lightning activity in the three main chimney regions. This topic deserves further study.

Figure 6 shows the comparison of normalized daily average SR intensity records for the globe (Figure 6a) with the normalized average SR intensity records of South America (Figure 6b), GLM daily flash rates (Figure 6c) and daily global mean land surface temperatures (NOAA CPC) and temperature anomalies (Berkeley Earth) (Figure 6d). The T_{AVG} and $T_{AVG,an}$ time series show a conspicuous minimum on 21 January, followed by the deep minimum of daily average SR intensity records on 22 January. The temperature anomaly time series also shows a maximum on 17 January, which is consistent with the SR intensity maximum on the same day. Land surface temperature anomaly maps (Movies S1 and S2) indicate that the observed minimum of the daily global means on 21 January involve equatorward transport of cold air from both poles in the same time frame. These observations suggest a thermodynamic origin of the global lightning variations indicated by the SR intensity records, as falling surface temperatures reduce two key drivers of thunderstorms: water vapor and CAPE (Williams, 2020). Based on GLD360 observations, the mean lightning response to temperature in one of the cold air outbreaks documented here is about 56% per °C, when averaged over the cold air mass in southern and central South America that appears to have its origin in Antarctica (Movies S1 and S2). Cold air outbreaks from a single pole and largely affecting a single hemisphere, are widely recognized (e.g., Hastenrath, 1996). It was quite surprising to the authors to find in this case the presence of concurrent outbreaks from two poles. This behavior is however consistent with the simultaneous presence of cold air anomalies in both the Arctic and the Antarctic (see surface air temperature maps at <https://climate.copernicus.eu/surface-air-temperature-maps>). This discovery was enabled by the interest in identifying the origin of an incontrovertible anomaly in global lightning activity.

There is an excellent agreement between the average SR intensity record corresponding to South America (Figure 6b) and the daily flash rates provided by the GLM (Figure 6c). It is noteworthy that the GLM flash counts, representing the entire Western Hemisphere, decline by approximately a factor of two from Jan 17 to Jan 22, in concert with the global quasi-invariant quantity (Figure 6a). The correlation coefficient between these two data sets is 0.93, which is much larger than the correlation between GLM and GLD360/ENTLN (0.69 and 0.63, respectively) (Figure S5 in Supporting Information S1). This result can be regarded as a further validation of our approach for producing quasi-global invariant SR intensity records characterizing individual chimneys.

In order to demonstrate the robustness of the introduced quasi-global invariant quantity in characterizing day-to-day changes in global lightning activity, Figure 7 presents the analysis of a second time interval from 1 to 31 January 2015. This second time interval (close to the solar cycle maximum) was chosen to check whether space weather-related processes, indicated by enhanced geomagnetic activity, could affect the SR-based quasi-invariant quantity. No obvious sign of cold air outbreaks was identified in the daily global mean land surface temperature records (not

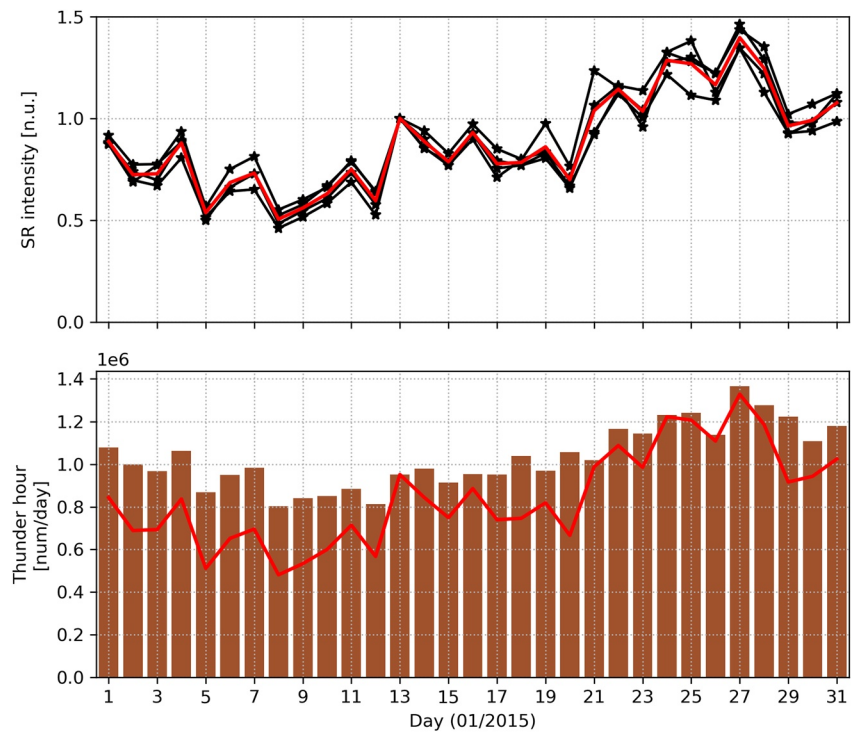


Figure 7. Comparison of normalized daily average SR intensity records (in normalized units, reference day: 13 January) from four stations (top) with the total daily numbers of Earth Networks Thunder Hours (bottom) in the 1–31 January 2015 time interval. In the top subplot black curves correspond to different SR stations while the red curve there shows the average of all records. The scaled version of the latter curve is also shown on the bottom plot. The correlation between the average SR intensity curve and thunder hours is 0.9.

shown here) for this period. SR data from 4 stations (ALB, BOU, HRN, NOR) on three continents were processed and compared with Earth Networks Thunder Hours which showed the highest correlation with the quasi-global invariant quantity in the original 19 days. The SR intensity curves from different stations track again very close to each other, and the correlation between the average SR intensity curve and thunder hours is 0.9. Another very encouraging result. It is to be noted that while in the second half of the month the two quantities indicate very similar levels of change (enhancement of global lightning activity), in the first half of the month the SR intensity indicates consistently lower activity than thunder hours. The reason for this discrepancy needs to be investigated further in the future.

4. Discussion

Although lightning is now recognized as an essential climate variable by the World Meteorological Organization (WMO) (Aich et al., 2018), the continuous monitoring of global lightning activity on the day-to-day timescale is severely limited as indicated by the apparently inconsistent global lightning distributions presented in Figure 2. Satellite observations do not provide global coverage on this timescale while the detection efficiency of available global ground-based lightning monitoring networks is limited, spatially uneven, and generally unknown (just as the location of the receiving stations is not freely accessible in the case of the GLD360 and ENTLN networks). Moreover, the detection efficiency of these networks is not stable but varies from day-to-day depending on the actual lightning distribution (see Figure 2 in Bitzer & Burchfield, 2016). Another important manifestation of this limitation is that even simple questions such as “which of the main lightning chimney regions was the most active on a given day” currently cannot be answered unambiguously (Figure 5). However, it should also be pointed out that the available technologies are constantly improving: for example, ENTLN has undergone a significant processor upgrade since the investigated period (Zhu et al., 2022), and geostationary lightning monitoring will soon be available for the European longitude sector as well (Holmlund et al., 2021).

Of the three global ground-based lightning detection networks studied here, the WWLLN network is clearly the least representative globally, and this is mainly related to its low detection efficiency in Africa (Figure 5)

(Williams & Mareev, 2014). With GLD360 reporting three times as many events as ENTLN (Figure 4) and showing better agreement with GLM data (Figure 2), it is likely that GLD360 was the most reliable and globally representative ground-based lightning detection network during the investigated period. However, based on our results, Earth Networks Thunder Hours is a very promising quantity for investigating day-to-day variations of global lightning activity (Figures 4 and 7). This is likely to be because the calculation of thunder hours remedies to some extent the differences in regional detection efficiencies.

Schumann resonance measurements offer a cost-effective way to monitor global lightning activity. However, SR intensity values do not provide direct information on the distribution of lightning activity at sub-continental scale. For this purpose we plan to use in the future an inversion algorithm aimed to infer the location and intensity of global lightning based on SR measurements (Dyrda et al., 2014; Nelson, 1967; Prácer & Bozóki, 2022; Prácer et al., 2019; Shvets & Hayakawa, 2011; Shvets et al., 2009, 2010; Williams & Mareev, 2014). The main difficulty in interpreting SR measurements is the complicated source-receiver distance dependence of the resonance field (see e.g., Nickolaenko & Hayakawa, 2002). It is a long-standing goal of SR research to derive a scalar quantity, a SR-based “geolectric index,” that characterizes the overall intensity of global lightning activity by eliminating this source-receiver distance effect (Holzworth & Volland, 1986; Sentman & Fraser, 1991). Our work followed the long recommended strategy of averaging the intensity of the two magnetic field components and as many resonance modes as possible (Nieckarz et al., 2009; Sentman & Fraser, 1991).

Several studies have previously analyzed SR intensity data from multiple stations (e.g., Bozóki et al., 2021; Füllekrug & Fraser-Smith, 1996; Price, 2000; Sentman & Fraser, 1991; Williams et al., 2021; Williams & Satori, 2004), but to the best of our knowledge, this is the first work that shows for many stations that summing the first three modes of the two magnetic components and averaging these values on a daily basis results in a quasi-global invariant quantity. This quantity shows a very good agreement with total (global) daily stroke rates provided by independent lightning observations and with the total daily numbers of Earth Networks Thunder Hours (Figures 4 and 7).

Our group sees great potential in comparing different geophysical parameters with the introduced quasi-global invariant quantity on the day-to-day time scale. The latter can be considered as an indicator of the day-to-day changes in the low-latitude atmospheric updraft, and thus it seems appropriate to investigate whether the upper layers of the atmosphere show considerable variability similar to the substantial day-to-day variability in global lightning activity. The work by Price (2000) can be regarded as such an approach where the author used an SR-based quantity as indicator for day-to-day changes in upper tropospheric water vapor. We also see it as an intriguing question whether there is a parameter (e.g., characterizing fluctuations in electron density) specific to the low-latitude ionosphere that correlates with the SR-based quantity we introduced.

At this point, some apparent limitations of the introduced SR-based quantity also need to be discussed. One major limitation is that in its current form, the quasi-global invariant quantity is not really suitable for studying longer time periods. The main reason for this statement is that on longer time scales, the source-observer distance effect associated with the seasonal north-south migration of global lightning activity causes significant changes in SR intensity (Nickolaenko et al., 1998) that are not corrected in the current form of the quasi-global invariant quantity. Further investigations are needed to clarify this likely difficulty, but it is recommended that the quantity introduced should only be used within a one-month period. Changes in the properties of the Earth-ionosphere cavity, that is, the propagation conditions of ELF waves on the even longer interannual time scale (Bozóki et al., 2021), are another challenge that needs to be addressed in the future. Shorter timescale changes in the properties of the Earth-ionosphere cavity associated with space weather, for example, connected with energetic electron precipitation (Bozóki et al., 2021), with geomagnetic storms (Pazos et al., 2019; Salinas et al., 2016), with solar proton events (Roldugin et al., 2003; Schlegel & Füllekrug, 1999), and with the solar rotation (Füllekrug & Fraser-Smith, 1996) can also bias the SR-based characterization of global lightning activity. However, in the present study there is no clear evidence of a significant space weather effect based on comparisons with independent lightning observations. This is in line with an important conclusion of Satori et al. (2016) that “*The inconspicuous response of SR amplitude/intensity to the most energetic solar events on record is consistent with theoretical considerations and provides additional indirect evidence that the SR intensity is primarily a record of the lightning activity within the Earth–ionosphere cavity.*”

If the quasi-invariant quantity were significantly affected by processes related to space weather, this influence is expected to occur during periods of increased geomagnetic activity indicated by the geomagnetic Kp index. The 19-day long period originally studied (13–31 January 2019) is close to the solar cycle minimum, when low

geomagnetic activity is expected in general. Accordingly, there is only one short, moderately disturbed period in the studied time interval, with a maximum Kp value of 4+ on the night of 24 January. It is expected that, in the presence of a space weather effect, SR intensity records from different stations will vary differently (as we expect the effect to be latitude-dependent) and/or deviate noticeably from independent lightning observations. No such effects are observed around 24 January. To gain further insight about this possible difficulty we selected the second time interval (1–31 January 2015) to be close to the solar cycle maximum and to include geomagnetically disturbed periods (max Kp: 6+ on 7 January). But even in this second time interval, we do not observe any indication of a significant space weather effect.

Observations in this study of global lightning on daily time scales have raised the interest in cold air outbreaks, a mechanism causing a global change in mean surface air temperature on the same time scale. We showed indications for near-simultaneous outbreaks from both Arctic and Antarctic, with influence in both the American and the African chimney. The chimney-by-chimney information on lightning activity presented in Figure 5 and augmented by GLM analysis (not shown) showed that the cold outbreak from Antarctica passed into Argentina and then proceeded to the eastern portion of the Amazon basin, where marked reduction in GLM-observed lightning was documented. This scenario is supported by surface skin temperature observations indicating that the cold outbreak first impacted the American chimney and then affected the African chimney as the temperature perturbation moved both equatorward and eastward.

In this study, our interest lies primarily in thermodynamic impacts on global lightning. However, given the recognized influence of aerosol on lightning activity (e.g., Williams, 2020), it should be noted that cold air outbreaks can also deliver cleaner polar air to lower latitude locations (e.g., Liu et al., 2019). The satellite-based method of estimating CCN concentration at cloud base height (Rosenfeld et al., 2016) was used to look for reductions in pollution linked with the equatorward motion of polar air in America and Africa, but no obvious signatures were identified.

Acknowledgments

This work was supported by the National Research, Development, and Innovation Office, Hungary-NKFIH, project numbers K138824 (T.B., S.G., S.P.), FK135115 (T.B., M.H.) and K125171 (M.H.). The work of T. Bozóki was supported by the ÚNKP-21-3 New National Excellence Program of the Ministry for Innovation and Technology from the source of the National Research, Development and Innovation Fund. The contribution of E. Williams and Y. Liu was supported by a grant from the US National Science Foundation (Grant # AGS-1945871 (“The GlobalCircuits Paradox”). M. Herein was supported by the János Bolyai Research Scholarship of the Hungarian Academy of Sciences. The authors thank I.R. Mann, D.K. Milling and the rest of the CARISMA team for data. CARISMA is operated by the University of Alberta, funded by the Canadian Space Agency. The authors wish to thank the World Wide Lightning Location Network (<http://wwlln.net>), a collaboration among over 50 universities and institutions, for providing the lightning location data used in this study. A. Potapov's contribution was supported by the project of the RF Ministry of Education and Science, and the data from obs. Mondy were obtained using the equipment of Center of Common Use “Angara” <http://ckp-rf.ru/ckp/3056>. Measurements at Vernadsky station were funded by “State Special-Purpose Research Program in Antarctica for 2011–2023” MES of Ukraine. The authors acknowledge the land surface temperature data provided by the NOAA PSL, Boulder, Colorado, USA (<https://psl.noaa.gov>).

5. Conclusions

In this paper we showed that by summing the intensity of the first three Schumann resonance (SR) modes of the two magnetic components and by averaging these values on a daily basis, a quasi-global invariant quantity can be obtained that can be used to investigate day-to-day changes in global lightning activity, supporting the earlier suggestion by Sentman and Fraser (1991). This quantity revealed significant variability in the overall intensity of global lightning activity that can occur within a few days and is likely explained by large-scale changes in land-surface temperatures related to cold air outbreaks. Independent global lightning data sets showed good agreement with the variations of the quasi-global invariant quantity. However, for the three main lightning chimneys on Earth the agreement among different lightning observations (including the SR invariant) is significantly worse than on the global scale, which underlines the need for improving the available observation methods and calculation techniques in this respect. An inversion algorithm that could infer the distribution and intensity of global lightning activity based on SR measurements would be very valuable to fill this important gap in our knowledge.

Data Availability Statement

Thunder hour data provided by Earth Networks, in collaboration with WLLN, are available at <http://thunder-hours.earthnetworks.com> (DiGangi et al., 2022). LIS/OTD data are available online (<https://ghrc.nsstc.nasa.gov/pub/lis/climatology/>) from the NASA EOSDIS Global Hydrology Resource Center Distributed Active Archive Center Huntsville, Alabama, U.S.A (Cecil, 2006). GLM data for this study were obtained through <https://console.cloud.google.com/storage/browser/gcp-public-data-goes-16> (GOES-R, 2018). Normalized daily average Schumann resonance (SR) intensity data are available at: <https://doi.org/10.5281/zenodo.7555111> (Bozóki et al., 2023).

References

- Adhitya, P., Nosé, M., Bulusu, J., Vichare, G., & Sinha, A. K. (2022). Observation of ionospheric Alfvén resonator with double spectral resonance structures at low latitude station, Shillong (dipoleL=1.08). *Earth Planets and Space*, 74(1), 169. <https://doi.org/10.1186/s40623-022-01730-2>
- Aich, V., Holzworth, R., Goodman, G., Price, C., & Williams, E. (2018). Lightning: A new essential climate variable. *EOS*, 99. <https://doi.org/10.1029/2018eo104583>. <https://eos.org/science-updates/lightning-a-new-essential-climate-variable>
- Albrecht, R. I., Goodman, S. J., Buechler, D. E., Blakeslee, R. J., & Christian, H. J. (2016). Where are the lightning hotspots on Earth? *Bulletin of the American Meteorological Society*, 97(11), 2051–2068. <https://doi.org/10.1175/BAMS-D-14-00193.1>

- Balsler, M., & Wagner, C. A. (1960). Observation of Earth-ionosphere cavity resonances. *Nature*, *188*(4751), 638–641. <https://doi.org/10.1038/188638a0>
- Barr, R., Llanwyn Jones, D., & Rodger, C. J. (2000). ELF and VLF radio waves. *Journal of Atmospheric and Solar-Terrestrial Physics*, *62*(17–18), 1689–1718. [https://doi.org/10.1016/S1364-6826\(00\)00121-8](https://doi.org/10.1016/S1364-6826(00)00121-8)
- Beggan, C. D., & Musur, M. (2018). Observation of ionospheric Alfvén resonances at 1–30 Hz and their superposition with the Schumann resonances. *Journal of Geophysical Research: Space Physics*, *123*(5), 4202–4214. <https://doi.org/10.1029/2018JA025264>
- Beirle, S., Koshak, W., Blakeslee, R., & Wagner, T. (2014). Global patterns of lightning properties derived by OTD and LIS. *Natural Hazards and Earth System Sciences*, *14*(10), 2715–2726. <https://doi.org/10.5194/nhess-14-2715-2014>
- Bitzer, P. M., & Burchfield, J. C. (2016). Bayesian techniques to analyze and merge lightning locating system data. *Geophysical Research Letters*, *43*(24), 12605–12613. <https://doi.org/10.1002/2016GL071951>
- Blakeslee, R. J., Lang, T. J., Koshak, W. J., Buechler, D., Gatlin, P., Mach, D. M., et al. (2020). Three years of the lightning imaging sensor onboard the international space station: Expanded global coverage and enhanced applications. *Journal of Geophysical Research: Atmospheres*, *125*(16), e2020JD032918. <https://doi.org/10.1029/2020JD032918>
- Blakeslee, R. J., Mach, D. M., Bateman, M. G., & Bailey, J. C. (2014). Seasonal variations in the lightning diurnal cycle and implications for the global electric circuit. *Atmospheric Research*, *135–136*, 228–243. <https://doi.org/10.1016/j.atmosres.2012.09.023>
- Boldi, R., Williams, E., & Guha, A. (2018). Determination of the global-average charge moment of a lightning flash using Schumann resonances and the LIS/OTD lightning data. *Journal of Geophysical Research: Atmospheres*, *123*(1), 108–123. <https://doi.org/10.1002/2017JD027050>
- Bozóki, T., Sători, G., Williams, E., Guha, A., Liu, Y., Atkinson, M., et al. (2023). Normalized daily average Schumann resonance (SR) intensity data from 13 to 31 January, 2019 [Dataset]. Zenodo. <https://doi.org/10.5281/zenodo.7555111>
- Bozóki, T., Sători, G., Williams, E., Mironova, I., Steinbach, P., Bland, E. C., et al. (2021). Solar cycle-modulated deformation of the Earth-ionosphere cavity. *Frontiers of Earth Science*, *9*. <https://doi.org/10.3389/feart.2021.689127>
- Brooks, C. E. P. (1925). The distribution of thunderstorms over the globe. *Geophys. Mem. London*, *24*, 147–164.
- Burgesser, R. E. (2017). Assessment of the world wide lightning location network (WWLLN) detection efficiency by comparison to the lightning imaging sensor (LIS). *Quarterly Journal of the Royal Meteorological Society*, *143*(708), 2809–2817. <https://doi.org/10.1002/qj.3129>
- Cecil, D. J. (2006). LIS/OTD 0.5 degree high resolution monthly climatology (HRMC). <https://doi.org/10.5067/LIS/LIS-OTD/DATA303>
- Cecil, D. J., Buechler, D. E., & Blakeslee, R. J. (2014). Gridded lightning climatology from TRMM-LIS and OTD: Dataset description. *Atmospheric Research*, *135–136*, 404–414. <https://doi.org/10.1016/j.atmosres.2012.06.028>
- Cecil, D. J., Buechler, D. E., & Blakeslee, R. J. (2015). TRMM LIS climatology of thunderstorm occurrence and conditional lightning flash rates. *Journal of Climate*, *28*(16), 6536–6547. <https://doi.org/10.1175/JCLI-D-15-0124.1>
- Chapman, F. W., Llanwyn Jones, D., Todd, J. D. W., & Challinor, R. A. (1966). Observation on the propagation constant of the Earth-ionosphere waveguide in the frequency band 8 kc/s to 16 kc/s. *Radio Science*, *1*(11), 1273–1282. <https://doi.org/10.1002/rdsl9661111273>
- Christian, H. J., Blakeslee, R. J., Boccippio, D. J., Boeck, W. L., Buechler, D. E., Driscoll, K. T., et al. (2003). Global frequency and distribution of lightning as observed from space by the optical transient detector. *Journal of Geophysical Research*, *108*(D1), ACL4-1–ACL4-15. <https://doi.org/10.1029/2002JD002347>
- Chronis, T., & Koshak, W. J. (2017). Diurnal variation of TRMM/LIS lightning flash radiances. *Bulletin of the American Meteorological Society*, *98*(7), 1453–1470. <https://doi.org/10.1175/BAMS-D-16-0041.1>
- Clayton, M., & Polk, C. (1977). Diurnal variation and absolute intensity of worldwide lightning activity, September 1970 to May 1971. In H. Dolezalek & R. Reiter (Eds.), *Electrical processes in atmospheres*. Verlag.
- Crossett, C. C., & Metz, N. D. (2017). A climatological study of extreme cold surges along the African highlands. *Journal of Applied Meteorology and Climatology*, *56*(6), 1731–1738. <https://doi.org/10.1175/JAMC-D-15-0191.1>
- DiGangi, E. A., Stock, M., & Lapierre, J. (2022). Thunder hours: How old methods offer new insights into thunderstorm climatology. *Bulletin of the American Meteorological Society*, *103*(2), E548–E569. <https://doi.org/10.1175/BAMS-D-20-0198.1>
- Dyrda, M., Kulak, A., Mlynarczyk, J., Ostrowski, M., Kubisz, J., Michalec, A., & Niecekarz, Z. (2014). Application of the Schumann resonance spectral decomposition in characterizing the main African thunderstorm center. *Journal of Geophysical Research: Atmospheres*, *119*(23), 13338–13349. <https://doi.org/10.1002/2014JD022613>
- Füllekrug, M. (2021a). Global lightning quanta. *Journal of Geophysical Research: Atmospheres*, *126*(9), e2020JD033201. <https://doi.org/10.1029/2020JD033201>
- Füllekrug, M. (2021b). Simulation of Earth-ionosphere cavity resonances with lightning flashes reported by OTD/LIS. *Journal of Geophysical Research: Atmospheres*, *126*(24), e2021JD035721. <https://doi.org/10.1029/2021JD035721>
- Füllekrug, M., & Fraser-Smith, A. C. (1996). Further evidence for a global correlation of the Earth-ionosphere cavity resonances. *Geophysical Research Letters*, *23*(20), 2773–2776. <https://doi.org/10.1029/96GL02612>
- Galejs, J. (1972). *Terrestrial propagation of long electromagnetic waves*. Pergamon.
- GOES-R Algorithm Working Group and GOES-R Series Program. (2018). NOAA GOES-R series geostationary lightning mapper (GLM) level 2 lightning detection: Events, Groups, and flashes [Dataset]. NOAA National Centers for Environmental Information. <https://doi.org/10.7289/V5KH0KK6>
- Goodman, S. J., Blakeslee, R. J., Koshak, W. J., Mach, D., Bailey, J., Buechler, D., et al. (2013). The GOES-R Geostationary Lightning Mapper (GLM). *Atmospheric Research*, *125–126*, 34–49. <https://doi.org/10.1016/j.atmosres.2013.01.006>
- Guha, A., Williams, E., Boldi, R., Sători, G., Nagy, T., Bór, J., et al. (2017). Aliasing of the Schumann resonance background signal by sprite-associated Q-bursts. *Journal of Atmospheric and Solar-Terrestrial Physics*, *165–166*, 25–37. <https://doi.org/10.1016/j.jastp.2017.11.003>
- Haldoupis, C., Rycroft, M., Williams, E., & Price, C. (2017). Is the “Earth-ionosphere capacitor” a valid component in the atmospheric global electric circuit? *Journal of Atmospheric and Solar-Terrestrial Physics*, *164*, 127–131. <https://doi.org/10.1016/j.jastp.2017.08.012>
- Hansen, J., & Lebedeff, S. (1987). Global trends of measured surface air temperature. *Journal of Geophysical Research*, *92*(D11), 13345–13372. <https://doi.org/10.1029/JD092iD11p13345>
- Hartjenstein, G., & Block, G. B. (1991). Factors affecting cold-air outbreaks east of the Rocky Mountains. *Monthly Weather Review*, *119*(9), 2280–2292. [https://doi.org/10.1175/1520-0493\(1991\)119C<2280:FACAOE>2.0.CO;2](https://doi.org/10.1175/1520-0493(1991)119C<2280:FACAOE>2.0.CO;2)
- Hastenrath, S. (1996). ‘Cold surges’, Section 7.9. In *Climate dynamics of the tropics*. Kluwer Academic Publishers.
- Heckman, S., Williams, E., & Boldi, R. (1998). Total global lightning inferred from Schumann resonance measurements. *Journal of Geophysical Research*, *103*(D24), 31775–31779. <https://doi.org/10.1029/98JD02648>
- Holmlund, K., Grandell, J., Schmetz, J., Stuhlmann, R., Bojkov, B., Munro, R., et al. (2021). Meteosat third generation (MTG): Continuation and innovation of observations from geostationary orbit. *Bulletin of the American Meteorological Society*, *102*(5), E990–E1015. <https://doi.org/10.1175/BAMS-D-19-0304.1>

- Holzworth, R., & Volland, H. (1986). Do we need a geoelectric index? *Eos, Transactions American Geophysical Union*, 67(26), 545–548. <https://doi.org/10.1029/EO067i026p00545-01>
- Holzworth, R. H., Brundell, J. B., McCarthy, M. P., Jacobson, A. R., Rodger, C. J., & Anderson, T. S. (2021). Lightning in the Arctic. *Geophysical Research Letters*, 48(7), e2020GL091366. <https://doi.org/10.1029/2020GL091366>
- Holzworth, R. H., McCarthy, M. P., Brundell, J. B., Jacobson, A. R., & Rodger, C. J. (2019). Global distribution of superbolts. *Journal of Geophysical Research: Atmospheres*, 124(17–18), 9996–10005. <https://doi.org/10.1029/2019JD030975>
- Hutchins, M. L., Holzworth, R. H., Brundell, J. B., & Rodger, C. J. (2012). Relative detection efficiency of the world wide lightning location network. *Radio Science*, 47(6), RS6005. <https://doi.org/10.1029/2012RS005049>
- Hutchins, M. L., Jacobson, A. R., Holzworth, R. H., & Brundell, J. B. (2013). Azimuthal dependence of VLF propagation. *Journal of Geophysical Research: Space Physics*, 118(9), 5808–5812. <https://doi.org/10.1002/jgra.50533>
- Jackson, J. D. (1975). *Classical electrodynamics* (2nd ed.). Wiley. Retrieved from <https://cds.cern.ch/record/100964>
- Kakad, B., Omura, Y., Kakad, A., Upadhyay, A., & Sinha, A. K. (2018). Characteristics of subpacket structures in ground EMIC wave observations. *Journal of Geophysical Research: Space Physics*, 123(10), 8358–8376. <https://doi.org/10.1029/2018JA025473>
- Kim, H., Hwang, J., Park, J., Miyashita, Y., Shiokawa, K., Mann, I. R., et al. (2018). Large-scale ducting of Pc1 pulsations observed by Swarm satellites and multiple ground networks. *Geophysical Research Letters*, 45(23), 12703–12712. <https://doi.org/10.1029/2018GL080693>
- Koloskov, A. V., Nickolaenko, A. P., Yampolsky, Y. M., Yu, C., Budanov, O. V., & Budanov, O. V. (2020). Variations of global thunderstorm activity derived from the long-term Schumann resonance monitoring in the Antarctic and in the Arctic. *Journal of Atmospheric and Solar-Terrestrial Physics*, 201, 105231. <https://doi.org/10.1016/j.jastp.2020.105231>
- Koloskov, O. V., Nickolaenko, A. P., Yampolski, Y. M., & Budanov, O. V. (2022). Electromagnetic seasons in Schumann resonance records. *Journal of Geophysical Research: Atmospheres*, 127(17), e2022JD036582. <https://doi.org/10.1029/2022JD036582>
- Kousky, V. E. (1979). Frontal influences on northeast Brazil. *Monthly Weather Review*, 107(9), 1140–1153. [https://doi.org/10.1175/1520-0493\(1979\)107<1140:FIONB>2.0.CO;2](https://doi.org/10.1175/1520-0493(1979)107<1140:FIONB>2.0.CO;2)
- Kulak, A., Kubisz, J., Klucjasz, S., Michalec, A., Mlynarczyk, J., Nieckarz, Z., et al. (2014). Extremely low frequency electromagnetic field measurements at the Hylaty station and methodology of signal analysis. *Radio Science*, 49(6), 361–370. <https://doi.org/10.1002/2014RS005400>
- Kulak, A., Mlynarczyk, J., Zieba, S., Micek, S., & Nieckarz, Z. (2006). Studies of ELF propagation in the spherical shell cavity using a field decomposition method based on asymmetry of Schumann resonance curves. *Journal of Geophysical Research*, 111(A10), A10304. <https://doi.org/10.1029/2005JA011429>
- Lanfredi, I. S., & de Camargo, R. (2018). Classification of extreme cold incursions over South America. *Weather and Forecasting*, 33(5), 1183–1203. <https://doi.org/10.1175/WAF-D-17-0159.1>
- Liu, Q., Chen, G., & Iwasaki, T. (2019). Quantifying the impacts of cold air mass on aerosol concentrations over North China using isentropic analysis. *Journal of Geophysical Research: Atmospheres*, 124(13), 7308–7326. <https://doi.org/10.1029/2018JD029367>
- Lupo, A. R., Nocera, J. J., Bosart, L. F., Hoffman, E. G., & Knight, D. J. (2001). South American cold surges: Types, composites, and case studies. *Monthly Weather Review*, 129(5), 1021–1041. [https://doi.org/10.1175/1520-0493\(2001\)129<1021:SACSTC>2.0.CO;2](https://doi.org/10.1175/1520-0493(2001)129<1021:SACSTC>2.0.CO;2)
- Lyons, W. A., Bruning, E. C., Warner, T. A., MacGorman, D. R., Edgington, S., Tillier, C., & Mlynarczyk, J. (2020). Megaflashes: Just how long can a lightning discharge get? *Bulletin of the American Meteorological Society*, 101(1), E73–E86. <https://doi.org/10.1175/BAMS-D-19-0033.1>
- Madden, T., & Thompson, W. (1965). Low-frequency electromagnetic oscillation of the Earth-ionosphere cavity. *Reviews of Geophysics*, 3(2), 211–254. <https://doi.org/10.1029/RG003i002p00211>
- Mann, I. R., Milling, D. K., Rae, I. J., Ozeke, L. G., Kale, A., Kale, Z. C., et al. (2008). The upgraded CARISMA magnetometer array in the THEMIS era. *Space Science Reviews*, 141(1–4), 413–451. <https://doi.org/10.1007/s11214-008-9457-6>
- Marchand, M., Hilburn, K., & Miller, S. D. (2019). Geostationary lightning mapper and Earth networks lightning detection over the contiguous United States and dependence on flash characteristics. *Journal of Geophysical Research: Atmospheres*, 124(21), 11552–11567. <https://doi.org/10.1029/2019JD031039>
- Marchenko, V., Mlynarczyk, J., Ostrowski, M., Kulak, A., Senchenko, O., Kubisz, J., et al. (2021). Study of a TGF associated with an Elve using extremely low frequency electromagnetic waves. *Journal of Geophysical Research: Atmospheres*, 126(3), e2020JD033070. <https://doi.org/10.1029/2020JD033070>
- Marchuk, R. A., Potapov, A. S., & Mishin, V. (2022). Synchronous globally observable ultrashort-period pulses. *Solar-Terrestrial Physics*, 8(2), 47–55. <https://doi.org/10.12737/stp-82202207>
- Marengo, J., Cornejo, A., Satyamurty, P., Nobre, C., & Sea, W. (1997). Cold surges in tropical and extratropical South America: The strong event in June 1994. *Monthly Weather Review*, 125(11), 2759–2786. [https://doi.org/10.1175/1520-0493\(1997\)125<2759:CSITAE>2.0.CO;2](https://doi.org/10.1175/1520-0493(1997)125<2759:CSITAE>2.0.CO;2)
- Markson, R. (2007). The global circuit intensity: Its measurement and variation over the last 50 years. *Bulletin of the American Meteorological Society*, 88(2), 223–242. <https://doi.org/10.1175/BAMS-88-2-223>
- Matsuda, S., Miyoshi, Y., Kasahara, Y., Blum, L., Colpitts, C., Asamura, K., et al. (2021). Multipoint measurement of fine-structured EMIC waves by Arase, Van Allen Probe A, and ground stations. *Geophysical Research Letters*, 48(23), e2021GL096488. <https://doi.org/10.1029/2021GL096488>
- Metz, N. D., Archambault, H. M., Shrock, A. F., Galarneau, T. J., Jr., & Bosart, L. F. (2013). A comparison of south American and African preferential pathways for extreme cold. *Monthly Weather Review*, 141(6), 2066–2086. <https://doi.org/10.1175/MWR-D-12-00202.1>
- Mlynarczyk, J., Bór, J., Kulak, A., Popek, M., & Kubisz, J. (2015). An unusual sequence of sprites followed by a secondary TLE: An analysis of ELF radio measurements and optical observations. *Journal of Geophysical Research: Space Physics*, 120(3), 2241–2254. <https://doi.org/10.1002/2014JA020780>
- Mlynarczyk, J., Kulak, A., & Salvador, J. (2017). The accuracy of radio direction finding in the extremely low frequency range. *Radio Science*, 52(10), 1245–1252. <https://doi.org/10.1002/2017RS006370>
- Murakami, T. (1979). Winter monsoonal surges over east and Southeast Asia. *Journal of the Meteorological Society of Japan*, 57(2), 133–158. https://doi.org/10.2151/jmsj1965.57.2_133
- Musur, M. A., & Beggan, C. D. (2019). Seasonal and solar cycle variation of Schumann resonance intensity and frequency at Eskdalemuir observatory, UK. *Sun and Geosphere*, 14(1). <https://doi.org/10.31401/SunGeo.2019.01.11>
- Nelson, P. H. (1967). *Ionospheric perturbations and Schumann resonance data*. Project NR-371-401. (PhD dissertation). Geophysics Laboratory, Massachusetts Institute of Technology.
- Neska, M., Czubak, P., & Reda, J. (2019). Schumann resonance monitoring in Hornsund (Spitsbergen) and Suwałki (Poland). *Publications of the Institute of Geophysics, Polish Academy of Sciences*, 425, 41–45. https://doi.org/10.25171/InstGeoph_PAS_Publs-2019-008
- Nickolaenko, A. P., & Hayakawa, M. (2002). *Resonances in the Earth-ionosphere cavity*. Kluwer.
- Nickolaenko, A. P., & Rabinowicz, L. M. (1995). Study of the annual changes of global lightning distribution and frequency variations of the first Schumann resonance mode. *Journal of Atmospheric and Terrestrial Physics*, 57(11), 1345–1348. [https://doi.org/10.1016/0021-9169\(94\)00114-4](https://doi.org/10.1016/0021-9169(94)00114-4)

- Nickolaenko, A. P., Satori, G., Zieger, B., Rabinowicz, L. M., & Kudintseva, I. G. (1998). Parameters of global thunderstorm activity deduced from long-term Schumann resonance records. *Journal of Atmospheric and Solar-Terrestrial Physics*, 60(3), 387–399. [https://doi.org/10.1016/S1364-6826\(97\)00121-1](https://doi.org/10.1016/S1364-6826(97)00121-1)
- Nieckarz, Z., Kulak, A., Zieba, S., Kubicki, M., Michnowski, S., & Baranskiaverage, P. (2009). Comparison of global storm activity rate calculated from Schumann resonance background components to electric field intensity E0Z. *Atmospheric Research*, 91(2–4), 184–187. <https://doi.org/10.1016/j.atmosres.2008.06.006>
- Pazos, M., Mendoza, B., Sierra, P., Andrade, E., Rodriguez, D., Mendoza, V., & Garduno, R. (2019). Analysis of the effects of geomagnetic storms in the Schumann resonance station data in Mexico. *Journal of Atmospheric and Solar-Terrestrial Physics*, 193, 105091. <https://doi.org/10.1016/j.jastp.2019.105091>
- Peterson, M., Mach, D., & Buechler, D. (2021). A global LIS/OTD climatology of lightning flash extent density. *Journal of Geophysical Research: Atmospheres*, 126(8), e2020JD033885. <https://doi.org/10.1029/2020JD033885>
- Plotnik, T., Price, C., Saha, J., & Guha, A. (2021). Transport of water vapor from tropical cyclones to the upper troposphere. *Atmosphere*, 12(11), 1506. <https://doi.org/10.3390/atmos12111506>
- Pracser, E., & Bozoki, T. (2022). On the reliability of the inversion aimed to reconstruct global lightning activity based on Schumann resonance measurements. *Journal of Atmospheric and Solar-Terrestrial Physics*, 235, 105892. <https://doi.org/10.1016/j.jastp.2022.105892>
- Pracser, E., Bozoki, T., Satori, G., Williams, E., Guha, A., & Yu, H. (2019). Reconstruction of global lightning activity based on Schumann resonance measurements: Model description and synthetic tests. *Radio Science*, 54(3), 254–267. <https://doi.org/10.1029/2018RS006772>
- Price, C. (2000). Evidence for a link between global lightning activity and upper tropospheric water vapour. *Nature*, 406(6793), 290–293. <https://doi.org/10.1038/35018543>
- Price, C. (2016). ELF electromagnetic waves from lightning: The Schumann resonances. *Atmosphere*, 7(9), 116. <https://doi.org/10.3390/atmos7090116>
- Price, C., Penner, J., & Prather, M. (1997). NOx from lightning: I. Global distribution based on lightning physics. *Journal of Geophysical Research*, 102(D5), 5929–5941. <https://doi.org/10.1029/96JD03504>
- Prince, K. C., & Evans, C. (2018). A climatology of extreme South American Andean cold surges. *Journal of Applied Meteorology and Climatology*, 57(10), 2297–2315. <https://doi.org/10.1175/JAMC-D-18-0146.1>
- Roldugin, V. C., Maltsev, Y. P., Vasiljev, A. N., Shvets, A. V., & Nikolaenko, A. P. (2003). Changes of Schumann resonance parameters during the solar proton event of 14 July 2000. *Journal of Geophysical Research*, 108(A3), 1103. <https://doi.org/10.1029/2002JA009495>
- Rosenfeld, D., Zheng, Y., Hashimshoni, E., Pohlker, M. L., Jefferson, A., Pohlker, C., et al. (2016). Satellite retrieval of cloud condensation nuclei concentrations by using clouds as CCN chambers. *Proceedings of the National Academy of Sciences of the United States of America*, 113(21), 5828–5834. <https://doi.org/10.1073/pnas.1514044113>
- Rudlosky, S. D. (2015). Evaluating ENTLN performance relative to TRMMLIS. *Journal of Operational Meteorology*, 3(2), 1120–20. <https://doi.org/10.15191/nwajom.2015.0302>
- Salinas, A., Rodriguez-Camacho, J., Portı, J., Carrion, M. C., Fornieles-Callejon, J., & Toledo-Redondo, S. (2022). Schumann resonance data processing programs and four-year measurements from Sierra Nevada ELF station. *Computational Geosciences*, 165, 105148. <https://doi.org/10.1016/j.cageo.2022.105148>
- Salinas, A., Toledo-Redondo, S., Navarro, E. A., Fornieles-Callejon, J., & Portı, J. A. (2016). Solar storm effects during Saint Patrick’s days in 2013 and 2015 on the Schumann resonances measured by the ELF station at Sierra Nevada (Spain). *Journal of Geophysical Research: Space Physics*, 121(12), 12234–12246. <https://doi.org/10.1002/2016JA023253>
- Satori, G. (1996). Monitoring Schumann resonances-II. Daily and seasonal frequency variations. *Journal of Atmospheric and Terrestrial Physics*, 58(13), 1483–1488. [https://doi.org/10.1016/0021-9169\(95\)00146-8](https://doi.org/10.1016/0021-9169(95)00146-8)
- Satori, G., Neska, M., Williams, E., & Szendroi, J. (2007). Signatures of the day-night asymmetry of the Earth-ionosphere cavity in high time resolution Schumann resonance records. *Radio Science*, 42(2), RS2S10. <https://doi.org/10.1029/2006RS003483>
- Satori, G., Williams, E., & Lempferger, I. (2009). Variability of global lightning activity on the ENSO time scale. *Atmospheric Research*, 91(2–4), 500–507. <https://doi.org/10.1016/j.atmosres.2008.06.014>
- Satori, G., Williams, E., Price, C., Boldi, R., Koloskov, A., Yampolski, Y., et al. (2016). Effects of energetic solar emissions on the Earth-ionosphere cavity of Schumann resonances. *Surveys in Geophysics*, 37(4), 757–789. <https://doi.org/10.1007/s10712-016-9369-z>
- Satori, G., & Zieger, B. (1999). El Nino related meridional oscillation of global lightning activity. *Geophysical Research Letters*, 26(10), 1365–1368. <https://doi.org/10.1029/1999GL900264>
- Satori, G., & Zieger, B. (2003). Areal variations of the worldwide thunderstorm activity on different time scales as shown by Schumann resonances. In S. Chauzy & P. Laroche (Eds.), *Proceeding of the 12th ICAE, global lightning and climate* (pp. 765–768). Versailles, France.
- Schlegel, K., & Fullekrug, M. (1999). Schumann resonance parameter changes during high-energy particle precipitation. *Journal of Geophysical Research*, 104(A5), 10111–10118. <https://doi.org/10.1029/1999JA900056>
- Schulzweida, U. (2021). *CDO user guide (version 2.0.0)*. Zenodo. <https://doi.org/10.5281/zenodo.5614769>
- Schumann, U., & Huntrieser, H. (2007). The global lightning-induced nitrogen oxides source. *Atmospheric Chemistry and Physics*, 7(14), 3823–3907. <https://doi.org/10.5194/acp-7-3823-2007>
- Schumann, W. O. (1952). Uber die strahlungslosen Eigenschwingungen einer leitenden Kugel, die von einer Luftschicht und einer Ionospharenhulle umgeben ist. *Zeitschrift fur Naturforschung*, 7(2), 149–154. <https://doi.org/10.1515/zna-1952-0202>
- Sentman, D. D., & Fraser, B. J. (1991). Simultaneous observations of Schumann resonances in California and Australia: Evidence for intensity modulation by the local height of the D region. *Journal of Geophysical Research*, 96(A9), 15973–15984. <https://doi.org/10.1029/91JA01085>
- Shvets, A. V., & Hayakawa, M. (2011). Global lightning activity on the basis of inversions of natural ELF electromagnetic data observed at multiple stations around the world. *Surveys in Geophysics*, 32(6), 705–732. <https://doi.org/10.1007/s10712-011-9135-1>
- Shvets, A. V., Hayakawa, M., Sekiguchi, M., & Ando, Y. (2009). Reconstruction of the global lightning distribution from ELF electromagnetic background signals. *Journal of Atmospheric and Solar-Terrestrial Physics*, 71(12), 1405–1412. <https://doi.org/10.1016/j.jastp.2009.06.008>
- Shvets, A. V., Hobara, Y., & Hayakawa, M. (2010). Variations of the global lightning distribution revealed from three-station Schumann resonance measurements. *Journal of Geophysical Research*, 115(A12), A12316. <https://doi.org/10.1029/2010JA015851>
- Strumik, M., Slominski, J., Slominska, E., Mlynarczyk, J., Blecki, J., Haagmans, R., et al. (2021). Experimental evidence of a link between lightning and magnetic field fluctuations in the upper ionosphere observed by Swarm. *Geophysical Research Letters*, 48(4), e2020GL091507. <https://doi.org/10.1029/2020GL091507>
- Tatsis, G., Sakkas, A., Christofilakis, V., Baldoumas, G., Chronopoulos, S. K., Paschalidou, A. K., et al. (2021). Correlation of local lightning activity with extra low frequency detector for Schumann resonance measurements. *The Science of the Total Environment*, 787, 147671. <https://doi.org/10.1016/j.scitotenv.2021.147671>

- Taylor, W. L. (1960). VLF attenuation for east-west and west-east daytime propagation using atmospherics. *Journal of Geophysical Research*, 65(7), 1933–1938. <https://doi.org/10.1029/JZ065i007p01933>
- Timofejeva, I., McCraty, R., Atkinson, M., Alabdulgader, A. A., Vainoras, A., Landauskas, M., et al. (2021). Global study of human heart rhythm synchronization with the Earth's time varying magnetic field. *Applied Sciences*, 11(7), 2935. <https://doi.org/10.3390/app11072935>
- Upadhyay, A., Kakad, B., Kakad, A., & Rawat, R. (2022). A statistical study of modulation of electromagnetic ion cyclotron waves observed on ground. *Journal of Geophysical Research: Space Physics*, 127(8), e2022JA030340. <https://doi.org/10.1029/2022JA030340>
- Virts, K. S., Wallace, J. M., Hutchins, M. L., & Holzworth, R. H. (2013). Highlights of a new ground-based, hourly global lightning climatology. *Bulletin of the American Meteorological Society*, 94(9), 1381–1391. <https://doi.org/10.1175/BAMS-D-12-00082.1>
- Wait, J. R. (1970). *Electromagnetic wave in stratified media*. The Institute of Electrical and Electronics Engineers Inc. New York: Oxford University Press.
- Welch, P. (1967). The use of fast Fourier transform for the estimation of power spectra: A method based on time averaging over short, modified periodograms. *IEEE Transactions on Audio and Electroacoustics*, 15(2), 70–73. <https://doi.org/10.1109/TAU.1967.1161901>
- Williams, E., Bozóki, T., Sători, G., Price, C., Steinbach, P., Guha, A., et al. (2021). Evolution of global lightning in the transition from cold to warm phase preceding two super El Niño events. *Journal of Geophysical Research: Atmospheres*, 126(3), e2020JD033526. <https://doi.org/10.1029/2020JD033526>
- Williams, E., Guha, A., Boldi, R., Christian, H., & Buechler, D. (2019). Global lightning activity and the hiatus in global warming. *Journal of Atmospheric and Solar-Terrestrial Physics*, 189, 27–34. <https://doi.org/10.1016/j.jastp.2019.03.011>
- Williams, E., Montanya, J., Saha, J., & Guha, A. (2023). Lightning and Climate Change, Chapter 15 in *Lightning Electromagnetics*. In V. In Cooray, M. Rubinstein, & F. Rachidi (Eds.), Vol 2. Institute of Engineering and Technology.
- Williams, E. R. (1992). The Schumann resonance: A global tropical thermometer. *Science*, 256(5060), 1184–1187. <https://doi.org/10.1126/science.256.5060.1184>
- Williams, E. R. (2005). Lightning and climate: A review. *Atmospheric Research*, 76(1–4), 272–287. <https://doi.org/10.1016/j.atmosres.2004.11.014>
- Williams, E. R. (2020). Chapter 2: “Lightning and climate change” Chapter 2 in book. In A. Piantini (Ed.), *Lightning interaction with power systems*. The Institution of Engineering and Technology.
- Williams, E. R., & Mareev, E. A. (2014). Recent progress on the global electrical circuit. *Atmospheric Research*, 135–136, 208–227. <https://doi.org/10.1016/j.atmosres.2013.05.015>
- Williams, E. R., & Sători, G. (2004). Lightning, thermodynamic and hydrological comparison of two tropical continental chimneys. *Journal of Atmospheric and Solar-Terrestrial Physics*, 66(13–14), 1213–1231. <https://doi.org/10.1016/j.jastp.2004.05.015>
- Yang, J., Zhang, Z., Wei, C., Lu, F., & Guo, Q. (2017). Introducing the new generation of Chinese geostationary weather satellites, Fengyun-4. *Bulletin of the American Meteorological Society*, 98(8), 1637–1658. <https://doi.org/10.1175/BAMS-D-16-0065>
- Zhu, Y., Stock, M., Lapierre, J., & DiGangi, E. (2022). Upgrades of the Earth networks total lightning network in 2021. *Remote Sensing*, 14(9), 2209. <https://doi.org/10.3390/rs14092209>